Line spectra of some giant and dwarf K-type stars

Koelbloed, D.

Publication date
1953

Table 1 Data of the Stellar Spectra

Star	Type	Spectrum			Plate No.	Date	Emulsion	Slit in 0.001 inch	Mean Hour Angle	Exposure Time	Seeing	Remarks
		Harvard	Morgan [1]	M.K.K. [2]								
						1929				(min)		
α Bootis	g	$K0$	$gK2$	$K2$ pec	17546	May 9	Process	0.5	$1^h\ 19^m$W	60	$1\frac{1}{2}$	
					17644	June 8	E 40	1.5	0 3 E	26	2	
					17645	June 8	E 40	1.5	0 18 W	8	2	
α Tauri	g	$K5$	$gK5$	$K5$ III	17922	Sept. 9	E 33	1.0	1 34 E	115	1+	
					18025	Oct. 1	E 40	1.5	1 48 E	39	1+	
					18026	Oct. 1	E 40	1.5	1 19 E	15	1+	
ξ Cygni	c	$K5$	$cK4$	$K5$ Ib	17692	July 5	E 40	1.5	0 27 E	161	$1\frac{1}{2}$	spectrum extends
					17787	Aug. 2	E 40	1.5	0 1 W	200	$1\frac{1}{2}$—1	to 4225 A
70 Oph. A	d	$K0$	$dK1$	$K0$ V	17744	July 18	E 40	1.5	0 2 E	87	$1\frac{1}{2}$	faint
					17763	July 29	E 40	1.5	0 47 W	240	$1\frac{1}{2}$—1	
61 Cygni A	d	$K5$	$dK5$	$K5$ V	17855	Aug. 20	E 40	1.5	0 44 W	90	0	very faint
					17867	Aug. 27	E 40	1.5	0 55 W	472	1—0	definition poor
					17867	Aug. 28	E 40	1.5	0 50 W	401	1—$1\frac{1}{2}$	
					17891	Sept. 3	E 40	1.5	0 54 W	410	2	spectrum extends
					17891	Sept. 4	E 40	1.5	0 38 W	400	1+—0+	to 4300 A

[1]) Ap. J. 88, p. 451, table 7.
[2]) W. W. Morgan, P. C. Keenan and E. Kellman: An Atlas of Stellar Spectra (1942).

As the resolving power shown on plate 17546 (Process) far exceeds those of the other plates, the equivalent widths derived for Arcturus are those of the Process plate only. For α Tauri all spectra have been combined into a mean spectrum in the way described below, giving different weights to the spectra according to their blackness on the photographic plate. This procedure has also been followed for ξ Cygni and 70 Ophiuchi. Only the mean spectra have been investigated. The spectra of ξ Cygni give in some small spectral regions mutual differences in density, perhaps defects in the photographic plates, rather than real variations of line intensities. Of the 61 Cygni plates only 17891 could be used for the measurements of line intensities. The exposure of this spectrum took two nights. Even today, it is the only spectrum taken, with this dispersion, of a $K5$ dwarf star.

The Zeiss step weakener was used for calibration until 8 September and replaced by the Hilger wedge after this date. Two developers were used, the Alkali developers until 30 June, and from then on a Borax developer. The slope of the characteristic curves depends slightly on the wave length and on the kind of developer used. The required corrections as given by Pannekoek [3] were taken into account, but are of little importance.

3. DERIVATION OF INTENSITY CURVES.

The spectra were registered with a Moll registering microphotometer of the Amsterdam Institute. The slit width of the microphotometer corresponds to 0.008 mm on the plate. The tracings were taken with an enlargement of 50 and 7 times. The smaller magnification was used

for drawing the background and for the detection of shallow depressions of molecular origin, manifesting themselves more clearly with small dispersion.

The large-scale tracings have been transformed into true intensity curves by the semi-automatic "Intensigraph", described by the author [14] elsewhere. This apparatus gives another magnification of 10 times, so that the final curve has a magnification of 500 times the dispersion. This size is convenient for our further reductions.

The intensity curves were taken on a logarithmic scale. As they are registered in this manner, it is easy to derive mean curves by placing different registrations on one another, without being obliged to adopt a background intensity beforehand. In the resulting curve the background can be put in afterwards and varied if necessary.

Of course the highest tops cannot be registered in this way and should, if wanted, be represented in the ordinary intensity scale. The intensities of the lines are derived by comparing the logarithmic intensity curves with a set of computed apparent profiles, drawn on the same logarithmic scale. The method will be explained below.

4. THE CONTINUOUS BACKGROUND.

A large source of error in the determination of equivalent width originates from the uncertainty where to draw the continuous background. This is already the case for solar-type stars, but in the ordinary photographic region of the *K* spectra the situation becomes much worse, especially for the giants. Observationally as well as theoretically it becomes difficult, where numerous lines blend together, to distinguish between the continuous spectrum and the line spectrum.

Van Albada [15] tried, for solar-type stars, to find corrections for the adopted wrong background by introducing them as additional parameters, determining his curves of growth. By comparing the computed blend intensities with the measured ones, equations were derived from which differential corrections for background intensity could be found by the method of least squares. However, this method gave, in some cases, improbably large corrections, probably owing to correlations between the different parameters. So this procedure will not be used here.

Neither could Minnaert's well-known method to find the background from the wings of strong lines be used, owing to the lack of unblended wings.

To fix the background for Arcturus, the only case where a Process plate was used, it seemed possible to compare the total absorption of different spectral regions computed with a preliminary background, with identical spectral regions of this star in the atlas of Hiltner and Williams [31]. This method has been successfully used by Walraven [2] when comparing Victoria sky spectra with the Utrecht Solar atlas. The dispersion of the Hiltner-Williams' atlas is roughly three times larger than of our spectra, so we may expect that the true background is approximated better in the atlas. Sixteen regions of about 15 A breadth each, between 4100 A and 4860 A were compared. From 4600 A to larger wave lengths, concordant results were obtained, but to the shorter wave lengths the deviations grew systematically till in the region near 4100 A our preliminary background was only 75 per cent of that of the atlas. K. O. Wright [16] reports that his Victoria measurements of Alpha Persei and Gamma Cygni give much smaller values for the equivalent widths in the ordinary photographic region than the corresponding ones obtained from tracings made with the direct-intensity microphotometer of Williams and Hiltner. He remarks, "It seems that the determination of the position of the continuous spectrum of these stars may offer greater difficulties than had been expected".

Also Milford [17], using the H. W. atlas for Arcturus, derives larger values for the total absorption of spectral regions than the values published by Shajn.

These instances clearly demonstrate the difficulties of the problem. For the other *K*-stars no intensity curves of spectra, taken with larger dispersion are available. As it is dangerous to apply a background correction, derived for a giant to a dwarf, it seemed better for our purpose — the comparison of giants and dwarfs — to treat the problem for all our stars with the same method. Therefore the reduction to the H.W. background was not carried out. The curve of growth of Arcturus for the shorter wave length region agreed better with the curve derived for the longer wavelengths, if our background was used, instead of the H.W. background. Yet, as long as one cannot explain the reported discrepancy, large uncertainties remain of course for $\lambda < 4600$ Å[1]).

For the background finally used the method adopted in principle was therefore the drawing of the continuous background as a smooth curve through the points of highest intensity, which will be defined below. This must be done with caution. In the first place there is an instrumental absorption band [3], caused by the glass of the prisms, resulting in a small depression in the region 4250—4600 A. In this case the background must follow the depression. Then, in the giants α Bootis and α Tau, there is a slowly varying depression in the continuum from 4106 A tot about 4240 A caused by *CN*-molecule absorption. The maximum depression [18] is near 4160 A. For α Tauri the maximum has an intensity of 76% of the undisturbed background intensity, for α Bootis we find 82%. If the band absorption takes place in the highest layers of the atmosphere or in a shell, both the stellar continuum and the absorption lines would be reduced in intensity in the same ratio. Then the observed equivalent width of the lines remain unaltered if we draw the background line again through the points of highest intensities within the disturbed region. If, however, the absorbing matter lies in the regions where the absorption lines are located, the sum of the absorption coefficients of the spectral line and of the disturbing agency should give the total depression. Perhaps, for these stars, where the molecule absorptions are not strong, the real case lies between these two extremes. As only medium strong and strong lines are measured in these regions, the results for log *W* differ at most 0.10 for a line, measured with both methods. Then it is sufficient to draw the background at an intensity midway between those corresponding with the line joining the points of highest intensity just outside the region 4106 A to 4240 A, and the line through the lowest points of the tracing within this region. Then applying the latter method, *i.e.* correcting the equivalent widths for the reduced molecule absorption, the deviation from the true case is smaller than about 0.05 in the log *W*, and therefore of little importance as compared with other sources of error.

Owing to the finite resolving power the observed spectral lines are broader than those of the true spectrum. Therefore the points of the highest intensity observed between the lines are practically always lying below the intensity of the "true" background. Only where there is a broad "window" the apparent intensity curve may occasionally reach the true value. Comparing the stellar "window" with the Utrecht Solar Atlas, it is always found that they correspond with rather broad continuous parts in the solar spectrum, but that they are always of much smaller extent, as was to be expected owing to the broader apparatus curve.

Table 2 gives the list of windows. The background finally adopted is such that its intensity may be about 2 per cent above the background in some of the windows, while for completely clear windows it coincides with it. It is seen that but few windows are common to all stars.

---

[1]) By using a model atmosphere, given by an effective gravity and a temperature at a certain optical depth, it is possible to compute the position of the theoretical background (Lewis and Liller[89]). As it is our purpose to find these parameters *independently*, such a method, however valuable, cannot be used here.

Table 2. List of "Windows".

70 Ophiuchi λ	61 Cygni λ	α Bootis λ	α Tauri λ	ξ Cygni λ
4221.0	4316.5	4087.5	4087.5	4316.5
4257.0	4335.9	4316.5	4279.2	4335.9
4316.5	4349.6	4345.3	4316.5	4349.4
4365.0	4445.0	4349.4	4328.4	4448.6
4499.8	4473.4	4504.2	4349.4	4608.3
4532.3	4521.6	4521.6	4448.5	4738.3
4559.3	4573.5	4559.2	4463.9	4951.5
4615.0	4615.0	4573.5	4521.5	
4618.2	4659.5	4608.3	4573.6	
4738.3	4711.0	4615.0	4608.3	
4819.7	4725.2	4621.1	4711.0	
4895.0	4735.1	4659.5	4879.5	
4944.1	4929.0	4711.0	4929.2	
	4945.0	4725.3	4943.5	
		4735.1		
		4750.5		
		4879.5		
		4915.5		
		4929.2		

5. AN ABSORPTION BAND OF UNKNOWN ORIGIN IN THE SPECTRUM OF 61 CYGNI.

An absorption feature in the spectrum of 61 Cygni of unknown origin has been found in the region 4770—4790 A.

Comparing the tracings with the Moll-microphotometer of 70 Ophiuchi and 61 Cygni we see a hump in the curve of the latter which is not present in the former (plate I tracings a and b). As this hump is present in all of the three spectra of 61 Cygni taken, it seems to be a real phenomenon in the spectrum of this star. The most likely explanation seems that the hump would be produced by molecule-band absorption. However we did not succeed in finding an identification. The band heads of *TiO* in that region are of the blue-green (α) system $c^3\pi - x^3\pi$ λ 4761 (2.0) and λ 4804 (3.1). These are strongly developed in the *M* giants, but are not seen in 61 Cygni. Even of the *TiO*-head λ 4955 (1.0), which is very strong in α Orionis (plate I tracing c), no trace is seen in the *K*5 dwarf.

With the aid of the curve of growth all absorptions of atom lines have been subtracted in order to obtain the undisturbed absorption phenomenon. The result is a rather symmetrical intensity distribution with a minimum intensity of 70 per cent of the continuous spectrum at 4780 A, extending from 4771 A to 4791 A.

Professor P. Swings was so kind as to ask Dr B. Rosen whether he could make any suggestion on the origin of this band. Dr Rosen found no good coincidences with spectra of diatomic molecules. Only *CuO* gives some coincidence. This molecule has a double band at 4772—4779 A. The identification of the other bands [19] of the same system (Bandes *A*) at 4917 A and 4635—4641 A is uncertain, partly by blending effects. In 61 Cygni there seems to be an indication of a depression between 4827—4846 A. In this region the double band 4828—4841 A, belonging to another system

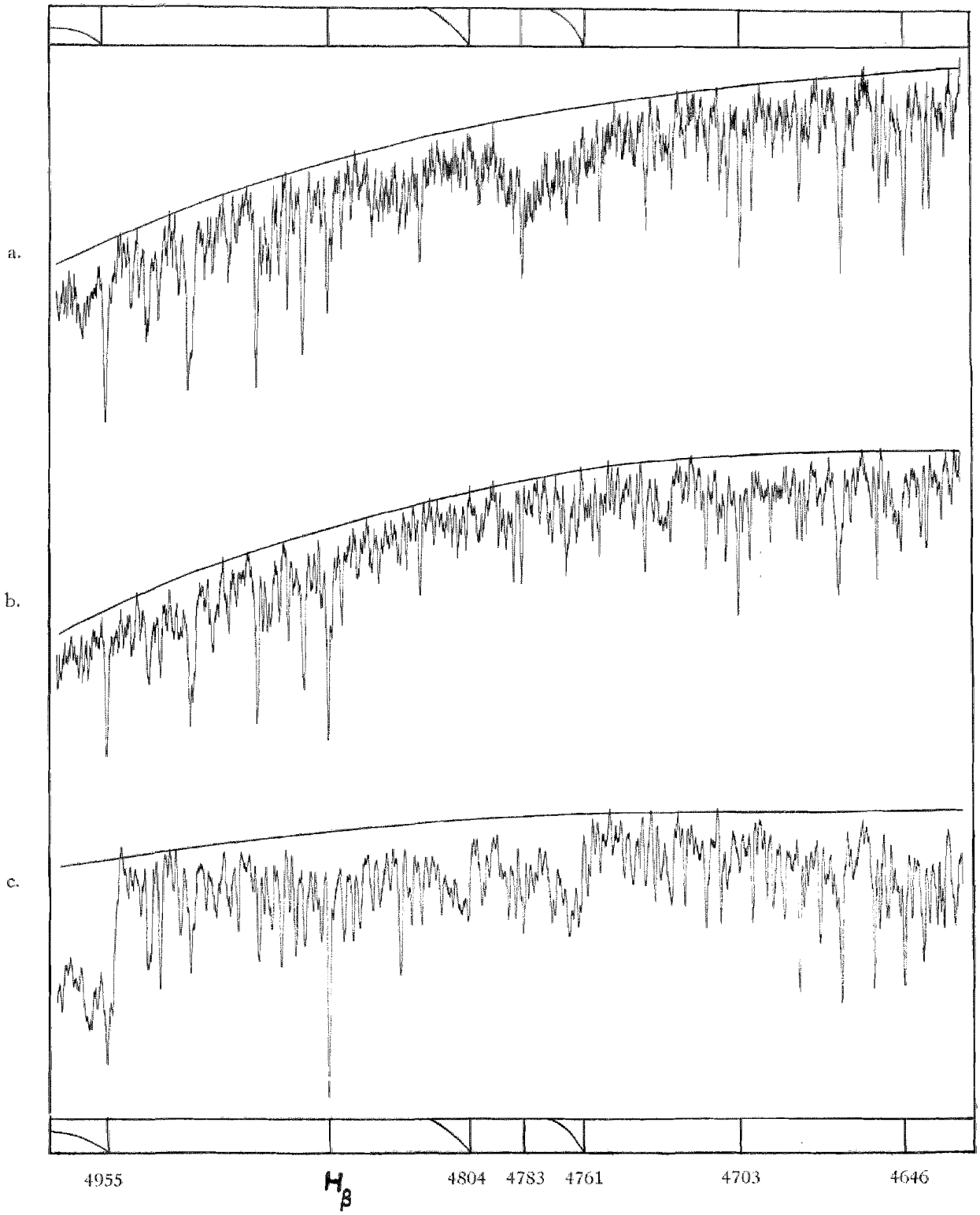

Plate I Density tracings (7×) made with the Moll microphotometer in the region $\lambda\lambda$ 4630—4976 A.

Tracing a, Plate No. 17891, 61 Cygni.
Tracing b, Plate No. 17763, 70 Ophiuchi.
Tracing c, Plate No. 17994, α Orionis.

(Bandes C) of CuO is situated. The only other band of this system, at 4684 A, may be there. However, the third system (Bandes B), with strong bands at 4708 A and 4853—4865 A in the laboratory, is definitely absent in the star.

6. THE DERIVATION OF EQUIVALENT WIDTHS.

a. The empirical line profile.

Our aim is to derive equivalent widths of single absorption lines. In the K stars, the blending by adjacent lines is very considerable in the photographic region; in fact, unblended lines are not found there. Therefore, the problem of finding the intensities for a great many lines can only be very approximately solved. In Amsterdam, the first treatment of blends in spectra of G-type stars by Pannekoek and Van Albada [20], consisted in computing theoretical line profiles, which were broadened afterwards by the instrumental curve or apparatus function, and the observed form of the blend could then be reconstructed by superposition of some of these single curves. The lines were identified by comparison with the solar spectrum, where they occur with a different intensity. This method was abandoned as being too cumbersome. Afterwards an analogous method was used by Walraven in a more practical form. This manner of treatment, which has much in common with the method followed here, was fully described by him [2] and Pannekoek [3]. Our first task consists in finding empirically the profiles of single lines in the intensity registrations. For a number of wave-length regions, all profiles, which seemed partly to consist of a single line, were drawn on a sheet of paper. The tops were placed on the same vertical line, in such a way that the background line was placed on a common horizontal base line. In this way an empirical set of curves of different intensity were formed from a number of fragments mostly consisting of left or right halves of profiles in the top regions. These sets served to construct mean empirical profiles, giving more weight to the parts of steepest descent, as probably these are real unblended parts. No difference in lineform could be detected between elements of different atomic weight. This must be due to the large instrumental profile combined with the turbulent motion of gases in the atmosphere. These mean sets often give a sufficient representation for the portion registered for the best plates up to 80 per cent of the background intensity. For higher intensities we have to use indirect methods. For the completion of the smallest profiles the *instrumental curve* must be known whereas for the determination of the wings of the larger lines the form of broadened *theoretical profiles* must be computed and fitted to the observed parts of the set of curves. The empirical sets were used as far as possible, only completed with theory if necessary.

b. The instrumental profile.

The results of the study of the instrumental profiles of the series of Victoria spectra, to which our K stars belong have already been discussed by Pannekoek[3] and Walraven[2] in two publications. The instrumental profile may be derived *from the comparison emission spectrum* of the iron arc. These lines were considered to have a negligible width. Of a large number of emission lines the widths at intensities 75, 50 and 25 per cent of the central intensity were measured. The characteristic curves, derived from the intensity marks, were used (see sections 1 and 2). Mean values for the widths at the three intensities mentioned were derived from one E 33 and seven E 40 plates: they are 21.0, 35.2 and 54.7 μ in the region of minimum width at 4250 A. Two Process plates gave the values 17.0, 27.9 and 44.3 μ. These numbers are valid for lines of medium strength (central intensities about 50 per cent).

We find for the minimum width (at λ 4250) of the iron comparison lines for our stars the values of the three last columns in the following table.

Table 3.

No.	Star	Emulsion	Slit	Width in μ		
				75%	50%	25%
17763	70 Oph	E 40	1.5	23.0	40.6	63.6
17891	61 Cyg	E 40	1.5	22.5	37.0	54.5
18025	α Tau	E 40	1.5	20.9	34.2	52.8
17546	α Boo	Process	0.5	17.5	27.8	43.9

The wings of the apparatus curve could be determined from the iron comparison spectrum on plate 18022 of Pannekoek's[3] series of plates, as here a strong continuous spectrum was visible. Thus, the faint extreme wings were brought above the threshold value so that measurement of intensity became possible. The results for the whole profile are given in the table 4 (valid for 4250 A).

Table 4. Instrumental curve determined from iron comparison lines.

Distance		Intensity	Distance		Intensity		Scale factors
μ	A.U.		μ	A.U.			
0	0.00	1.00	35	0.35	0.125	λ 4100	1.14
5	0.05	0.928	40	0.40	0.087	λ 4200	1.00
10	0.10	0.760	45	0.45	0.064	λ 4300	1.01
15	0.15	0.585	50	0.50	0.047	λ 4400	1.07
20	0.20	0.415	60	0.60	0.030	λ 4500	1.16
25	0.25	0.280	70	0.70	0.020	λ 4600	1.25
30	0.30	0.186	80	0.80	0.014	λ 4700	1.35
						λ 4800	1.45

The instrumental curve changes its shape with wave length. We assume that for other wave lengths the shape of the profile can be reduced to the standard form by only multiplying the abscissae expressed in mm by a constant which we call the scale factor. Table 4 gives the scale factor, derived by comparing lines of various wave lengths in the comparison spectrum of the plates of table 3, as a function of the wave length.

An uncertainty remains in the results of tables 3 and 4. It was experimentally shown[3] for the emulsions used that short exposures had a less steep characteristic curve than the long ones. As the comparison spectra were exposed for only a few seconds and the calibration marks for several minutes, it seems possible that, using the characteristic curve derived from the latter, the comparison lines turn out too broad. The width of the emission lines measured at a fixed percentage of the value of the central intensity, depends in a systematic way on the value of the central intensity. This shows that indeed variation of slope and possibly other photographic effects are at work. Moreover, the average factor 0.94, used to adapt the characteristic curve derived from the calibration bands of a few minutes' exposure to the stars of an exposure of the order 1 hour, may be in error for the very long exposure of the *K* dwarfs. Therefore, there may be some uncertainty as to how far the apparatus function derived from the comparison spectrum is valid for the spectrum of the

star. Although some information of a qualitative character may be obtained from theoretical investigations[15] on the variation of slope and from Kron's[3] empirical rules, yet these considerations cannot give us quantitative data for a proper reduction. From this reasoning it seems probable that one finds too high equivalent widths for lines of small depths if the results of the comparison spectrum are used.

The determination of the shape of the apparatus curve *from stellar lines of medium strength* is very uncertain, especially in the *K* stars. A priori, we do not know the true profiles so it is not possible to compute the apparatus function from the observed and the true profiles. Yet it is possible for the Process plate of Arcturus to derive some empirical information about the instrumental profile from the stellar absorption lines, which may serve as a rough check of the results given in tables 3 and 4. For the region 4420—4642 A, the widths of the stellar lines at line depth 75 and 50 per cent of the central depth R_c were measured for 20 absorption lines, which seemed free of companions. In fig. 1 the central depth is plotted as a function of the line width. Extrapolated to central depth zero (very faint absorption lines) the curves must yield the instrumental width. From table 4 we derive the instrumental width from emission lines for the mean wave length in the observed region, which are placed as crosses at depth zero in the diagram. The agreement of the two methods seems sufficient. For the other stars the spread of the points precludes any conclusion.

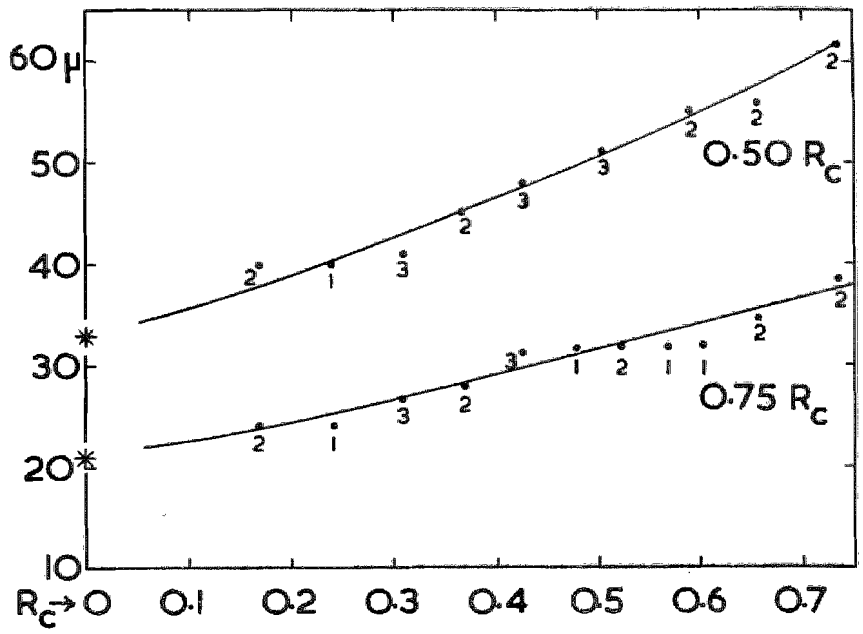

Fig. 1. Comparison of the instrumental widths, derived from the absorption lines of the Arcturus spectrum, with those obtained from the emission comparison spectrum (*).
The numbers at the dots represent the numbers of absorption lines used.

Therefore, the only thing we can do is to adopt the data of tables 3 and 4, but we must keep in mind that systematic errors may occur in the weak lines, which are exactly of most importance for constructing the curve of growth. The intensity of the weak lines in these spectra are for a large part obtained from residuals left by larger lines. These residuals are insufficient to fix the shape of the faint lines. Therefore, the error in the adopted form of the instrumental profile is reflected fully in the equivalent width.

c. The theoretical profile.

For the wings of medium and strong lines we have to compute first the theoretical profiles by adopting plausible parameters.

The derivation of the theoretical or "true" profile consists in:

1. determining the coefficient of line absorption as a function of damping (radiation and collision damping) and Doppler broadening.
2. the derivation of the true profile from the coefficient of line absorption and a number of parameters depending on the structure of the atmosphere.

1. *The coefficient of line absorption* with damping and Doppler broadening combined is given[21] by

$$\frac{k(v)}{k_\circ} = \frac{a}{\pi}\int_{-\infty}^{\infty} \frac{e^{-y^2}\,dy}{a^2+(v-y)^2} \tag{1}$$

where $k(v)$ is the selective absorption coefficient per atom, for the wave length λ with

$$v = \frac{\lambda_\circ - \lambda}{\Delta\lambda_D}$$

In this expression $\lambda_\circ$ is the wave length of the centre of the line and $\Delta\lambda_D = \frac{\lambda}{c}\sqrt{\frac{2RT}{\mu}}$ the Doppler width or if there is a turbulent velocity V_t superposed

$$\Delta\lambda_D = \frac{\lambda}{c}\sqrt{\frac{2RT}{\mu} + V_t^2}. \tag{2}$$

The absorption coefficient at the centre of the line is $k_\circ$ and

$$a = \frac{\Delta\lambda_N}{\Delta\lambda_D} \tag{2a}$$

in which $\Delta\lambda_N$ is the damping width expressed in Angström units. For a classical oscillator

$$\Delta\lambda_{Ncl} = 0.59\times 10^{-4} A. \tag{2b}$$

It should be noted that in this case the a used by Unsöld is twice this a. For a number of a values the integral (1) was computed by Hjerting[22]. His tables have been used. For $a = 0.001$ Van der Held's[23] formula has been taken, as this value does not occur in Hjerting's tables.

2. *The true profile of an absorption line.*

The residual intensities for points on the line profile can only be derived from a detailed knowledge of atomic constants and the physical conditions in the various depths of the stellar atmosphere. Many approximate solutions of this intricate problem have been given. We do not know a priori the structure of the atmosphere of the star we wish to study, nor is it possible to take account of the various ways of line formations of different lines. In view of the rather large apparatus function our demands are not high and therefore it suffices to adopt the simple approximate formula for the residual intensity

$$r = \frac{1}{1+\tau_\lambda} \tag{3}$$

to be used for all lines. Here $\tau_\lambda = N k_\nu$ is the selective optical depth, N the number of atoms capable of absorbing the line and k is the monochromatic absorption coefficient given by (1).

Comparing with Unsöld's[21] formula for the Schuster-Schwarzschild model (64.8) and for the Milne-Eddington model (65.23) both valid for pure scattering, we note that up to residual intensities of 40 per cent the three formulae give nearly the same values. So for completing our empirical curves with wings the adopted formula proves sufficient.

d. The theoretical apparent profile.

The apparent profile $F(x)$ of a spectral line is produced by broadening the true profile $W(x)$ by the apparatus function $A(x)$.

$F(x)$ is given by

$$F(x) = \int_{-\infty}^{\infty} W(y)\, A\,(x-y)\, dy \tag{4}$$

The writer obtained for a variety of A and W values the F profiles by means of the optical method described by Burger and Van Cittert[24]. The practical details have been described by A. Pannekoek[3].

As is easily verified, the true profile of a spectral line of a given equivalent width ,expressed in Angström units, does not vary much over the region studied (4100—4800 A). It is sufficient therefore to work with one set of theoretical profiles computed for 4400 A.

As the number of Angströms per mm varies strongly with λ, the scale factor expressed in mm in table 4 must be transformed to the factor with the Angström as unit. The scale factors expressed in Angström units become as given in the last column of table 5, the profile at λ 4250 being again the standard.

An easy method of broadening with the aid of Voigt profiles was published by Van de Hulst[25] and a table and graph for practical use was given by him and Reesinck[26]. As a check of our results, but also as a quick independent method the Voigt-profile method was used. This method cannot be used for the theoretical profiles with flat tops, but is it very well applicable to the apparatus profile. It is also applicable to the theoretical profiles broadened with the apparatus curve, in other words to our apparent theoretical profile, and may therefore serve to derive this profile for any wave length from the standard profile at λ 4250.

Table 5.

λ	μ per A	Scale factor in mm	Scale factor in A
4100	147	1.14	0.91
4200	127	1.01	0.94
4250	118	1.00	1.00
4300	110	1.01	1.08
4400	97	1.07	1.30
4500	85	1.16	1.61
4600	76	1.25	1.94
4700	69	1.35	2.31
4800	62	1.45	2.76
4900	57	1.55	3.21

For a description and use of the method, we refer to both papers.

e. The analysis of the blends.

If the broadening influence of the apparatus can be neglected, the observed blends are called *real*, they originate in the atmosphere of the star. Then the *sum of the optical depths* of all lines

composing the blend *determines the residual intensity*. The analysis of such blends has been treated by several investigators, most recently by the Utrecht observers[27]. The problem is highly complicated among others by the different atmospheric models valid for the different atoms or ions.

Walraven[2] adopts for δ Cephei-spectra, taken with the same dispersion and with the same instrument, the method of analysing the observed blends *as if they were real blends*. He takes formula (3) for the computation of the residual intensity, which in the case of a blend is given by taking for τ the sum of the optical depths of the components.

In practice the disentanglement of a blend is done graphically. As an instance we consider a blend composed of a strong line with a weak one on its wing. For the strong line the whole profile is found by comparing its undisturbed part with a set of theoretical — or semi theoretical apparent profiles (ordinate = log r). To this end the intensity curve of the spectrum is put on the set, which is illuminated from below. Then the complete profile of the strong line is drawn (cf. fig. 2), so that in the disturbed region the log r's of the strong line and of the sum of both components are known. For a certain wavelength, the optical depths, corresponding with both r's, are read from a vertical scale, giving τ as a function of log r. The difference between both optical depths is the optical depth of the weak line. The log r of the undisturbed weak component is found by again using the vertical scale. By repeating this method for several wave lengths, the profile of the undisturbed weak line becomes known. Then a theoretic apparent profile of the set is fitted as well as possible and the corresponding equivalent width is read from the set. For more details we refer to Walraven's paper.

This procedure was used also for our K-spectra. In view of the large apparatus curve, it must be considered only as a rough approximation especially for heavily blended lines of medium strength, which are therefore omitted. A real improvement of the results can only be expected from spectra taken with larger resolving power.

7. THE CATALOGUE OF LINE INTENSITIES.

The catalogues for the atomic lines (table 6, p. 83) and for the ion lines (table 7, p. 90) give log W/λ, in units of 10^{-6}, where the equivalent width W is expressed in Angstrom units. The weight is given according to the degree of blending. Weights 3 and 4 are given to lines which are for a large part indicated in the registrations. For lower weights the intensity given is in an increasing way a product of the intensity residuals left by the stronger lines. As faint lines of atomic or molecular origin contribute in an unknown way to these residuals, the faint lines measured may have the tendency to become somewhat too strong. Although the aim was to obtain as many lines as possible, many heavily blended parts had to be left unused, owing to the great complexity, for instance the region of the G band in all stars. The spectra extend a good deal beyond λ 4770 towards the longer wave length. Yet, this limit was chosen, because the apparatus curve became too wide there.

For the identification of element and wave length the Revision of Rowland's table of solar wave lengths has been used together with Hacker's[28] identification list for the Arcturus spectrum [1]). For the $K5$ stars this list is also of much value. TiO absorption is still negligible in Aldebaran and 61 Cygni. In ξ Cygni an intensity drop (CN) abruptly sets in at 4606 A (Δ log I = 0.05), diminishing towards the longer wave lengths (to about 4500 A). The drop was dealt with as a wing of a neighbouring line, and the equivalent widths were corrected as in this case[29]. For the spectrum of this star also, Hacker's list was used. The extensive list of Davis[30] for the M-giant

[1]) Very recently an excellent table of wave-lengths and identifications of spectral lines for K Giants ($\lambda\lambda$ 4000—5000 A) given by L. Gratton appeared in the Ap. J. **115**, 346, 1952. As our work was finished already, we did not use it.

β Pegasi might have served for further identifications, but the quality of our spectrum did not warrant the immense task of accounting for all details. Therefore, we only give our determinations of intensities of the spectral lines in Hacker's list.

A sufficient fit of the broadened theoretical profiles to the empirical set of curves was obtained with the parameters $a = 0.003$ and $\Delta\lambda_D = 0.065$ A for α Bootis. The fit can be improved by a slight adjustment of the scale factor which is not exactly known. For the giants α Tauri and ξ Cygni $a = 0.001$ and $\Delta\lambda_D = 0.1$ A was tried. Both dwarfs show nearly the same empirical curves. Adopting $a = 0.02$ and $\Delta\lambda_D = 0.03$ A which leads to a damping factor $\Delta\lambda_N$ ten times the value for radiation damping, as is the case for the sun, we obtain too broad profiles. By taking $\Delta\lambda_D = 0.04$ A and $a = 0.01$ a better fit was obtained.

The three strong iron lines λ 4383.5, 4404.8 and 4415.1 were measured direct on the intensity diagram, i.e. without the help of broadened theoretical profiles.

8. THE HYDROGEN LINES.

Of the hydrogen lines only the $H\beta$ and the H_γ were studied, as the spectral region of the higher members of the Balmer series is too faint on our plates.

In the *giants* $H\beta$ is relatively little blended at the side of the longer wave lengths. The profiles can be seen up to a depth of 80 per cent of the continuous background intensity. In the other wing the iron line 4859.85 A strongly disturbs the profile. Therefore for the giants a symmetrical profile, one half of which is given by the red wing, was adopted for the derivation of the equivalent width. For ξ Cygni we find perhaps a somewhat too small equivalent width, if measured in this manner, because the wing at the blue side seems a little stronger.

For the *dwarfs* the determination of the intensity of $H\beta$ is more difficult owing to the stronger blending. Only approximate intensity values can be obtained after correcting for the disturbing neighbouring lines. With the help of Allen's solar log *Nf* for 4859.85 A (*Fe*), corrected for temperature, and by using our curves of growth (see Section 10) we determined the intensity at this wave length that remained after correction for the absorption of this line. This intensity gives the minimum intensity of $H\beta$ at this wave length. For the disturbing components at the other wing the *Nf* values are too uncertain for such a correction. The results for log *W* are given in table 8. For the dwarfs a small decrease and for the giants a small increase with decreasing temperature seems indicated for $H\beta$. The supergiant has the strongest lines.

Table 8. The table gives log W for Hβ and Hγ (Unit 1A)

Line	Observer	α Boo gK_2	α Tau gK_5	ξ Cyg cK_5	70 Oph. dK_1	61 Cyg. dK_5	Reference	Dispersion in A/mm
$H\beta$	Koelbloed	0.08	0.13	0.19	0.05	9.9		14
$H\gamma$		9.90	9.69	0.15	—	9.48		10
$H\beta$	E. G.	0.02	—	—	—	—	Solar Ph. Obs.	
$H\gamma$	Williams	0.13	0.26	—	—	—	Cambridge II, part II, 1932	25 to 28
$H\beta$	Thackeray	0.11	0.15	0.15	0.08	—	M. N. 109, 452, '49	51
$H\beta$	Elvey	0.17	9.99	—	0.38	—	Ap. J. 71, 198, '30	16
$H\beta$	Wright	0.01	—	—	—	—	Dom. Obs. Victoria Publ. VIII, 290, '50	7

For H_γ the difficulties of blending effects and of the continuous background are still greater than for $H\beta$. Only the top regions are observable on our plates. *A priori* we cannot adopt the shape of the empirical set, derived from lines of other elements. However the profile of H_γ in α Boo, for instance, does not give the impression of being much broader than the strong lines of other elements. As an example we give in figure 2 the H_γ complex for α Tauri. After disentangling the intensity curve with the empirical set of profiles, the disturbing lines have been drawn in the figure, and the intensity left for H_γ is given by dots. Of the set of profiles the one passing through the top of H_γ is chosen and represented by the dashed line. According to Verwey the Stark effect does not give appreciable broadening for temperatures below 3600°. Moreover, the apparatus curve is broad and the turbulent velocity in the giants is high, about equal to the thermal velocity of hydrogen. These facts tend to diminish the difference between the profiles of H_γ and of the other elements. Adopting the set of empirical profiles derived for the other elements for the hydrogen lines, we find for log W the values given in table 8. Since the difference in thermal motion has been neglected, we find *minimum* values for this reason. For 70 Oph the blending is too severe to give an estimate.

9. COMPARISON OF THE EQUIVALENT WIDTHS WITH THOSE OF OTHER OBSERVERS.

a. The hydrogen lines.

In table 8 we also give the few photometric results obtained by other observers. The values given for $H\beta$ by Thackeray are in good agreement with our determinations. For the line $H\beta$ of the dwarf 70 Oph Elvey gives a much larger value than our estimate, even larger than for the giants. If we had not taken into account the blending lines, we should also have found a much larger value. If we compare our result with Williams' measurements, the largest difference is found for H_γ in α Tau. The cause of the discrepancy is at once seen if we draw the profile given by Williams in our figure 2 (dashed line). The top intensities of H_γ (uncorrected for the apparatus broadening) coincide for both observers. However the whole line complex is ascribed by him to H_γ, which is unlikely in view of the strong neighbouring lines. Our results for W of the *Cr* lines λ 4339.46 and λ 4339.72 are in fair agreement with the values computed with the reduced log Nf (Allen) in combination with the curve of growth, valid for *Cr* lines measured in less disturbed spectral regions.

This example clearly shows the danger we encounter if spectra taken with small dispersion are used. Also our dispersion is too small to give reliable results for H_γ. Even with larger dispersion physical blending will still remain. It should be remembered that the problem of unravelling the complex of lines of very different excitation and ionization potential, as is the case here, is much more involved owing to stratification effects than our approximate method [88]. A detailed atmospheric model, which should also explain the abnormal strength of the hydrogen lines in the red giants, is necessary to solve the problem in a satisfactory way.

b. Comparison of equivalent widths in the spectrum of Arcturus with those of other observers.

As was remarked in section 4, the position of the curve for the continuous spectrum of Arcturus for $\lambda > 4600$ A in the Hiltner-Williams atlas coincides with our determination. For comparison of individual line intensities 22 lines in the region λ 4581—4747, which seemed unblended on the tracings, were measured in this atlas, adopting triangular profiles. In fig. 3 the

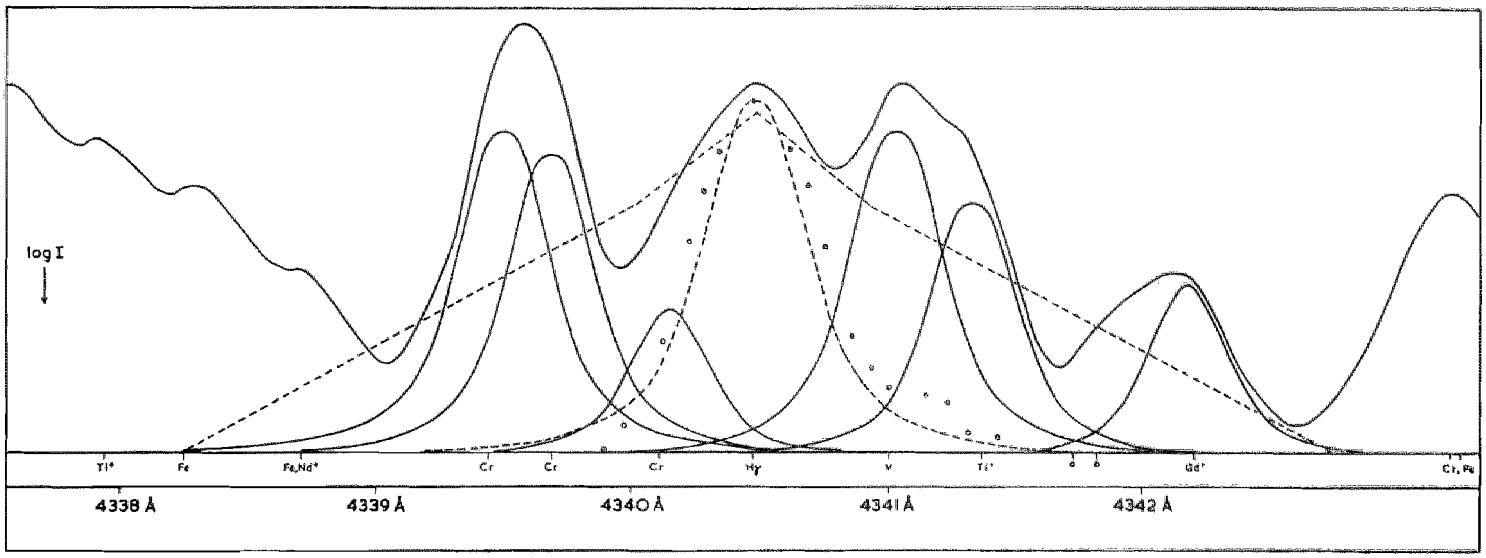

Fig. 2. The region near $H\gamma$ in the spectrum of Aldebaran. The dots represent the depths left for $H\gamma$, after correcting the observed intensity curve for the blending of neighbouring lines. The outer dashed line represents the $H\gamma$ profile, given by E. G. Williams.

log W values of the atlas were plotted against our measurements. The mean difference Δ log W is only 0.02, our lines being slightly stronger. For blended lines the agreement will, of course, be less satisfactory. The dispersion of the H-W atlas in this region corresponds to 4.3 A/mm on the photographic plate.

We also carried out a comparison with Wright's[13] measurements in spectral region 4657—4770 A, which is common to both investigations. In this region our dispersion is 14.5 A/mm against 7.0 A/mm of Wright. For identification we used Hacker's list 7 (4 A/mm). Only those lines were used by us, where Hacker gives *one* component. Only 9 lines were in common, they were plotted in fig. 4. Our lines are systematically stronger, as is often the case for smaller dispersion. It is likely that a large part of the difference may be explained by the better correction for blending in the case of the larger dispersion. For 3 lines Wright also gives one component. For them the mean Δ log $W = 0.06$. For 4 lines, where Wright gives two or more components, the mean Δ log $W = 0.10$. For the two largest deviations λ 4753.96 and 4757.50 indicated by crosses, Hacker's and Wright's identifications disagree, *viz.* Mn (Hacker) against *V, Mn* (Wright) and *Fe* (Hacker) against *V, Fe, Cr* (Wright) respectively. If these components, measured by Wright, are supposed to be of equal intensity the deviations may be understood.

10. THE CURVES OF GROWTH.

To obtain information about electron pressure, temperature, turbulence and abundances in the stellar atmosphere, it is necessary to derive the curve of growth, i.e. the relation between the line strength and the effective number of absorbing classical oscillators Nf per cm^2, where N is the "total number of absorbing atoms per 1 cm^2 above the photosphere" and f is the oscillator strength. As for a large number of lines the theoretical or laboratory intensities are lacking, Allen's[32] curve of growth of the sun, together with his solar line intensities, will be used to obtain Nf-values for the sun. Allen's solar values were obtained with his table 3, taking into account the differences

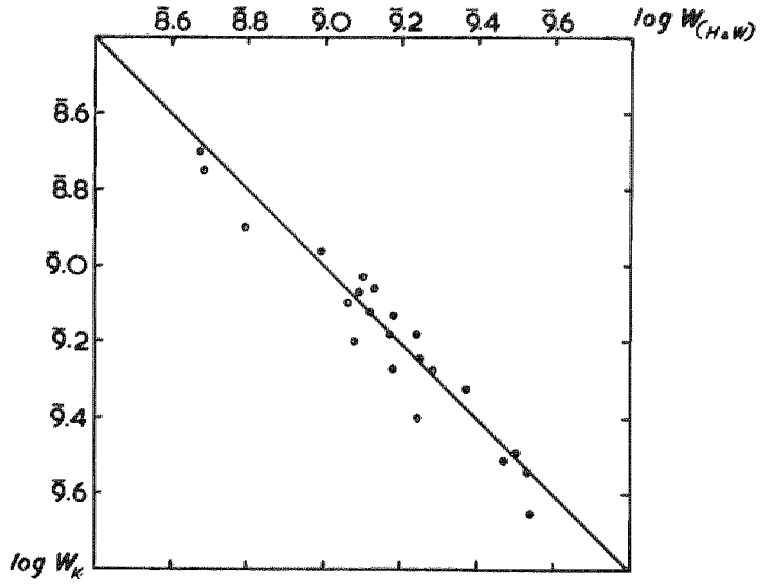

Fig. 3. Comparison of our equivalents widths (W_K), derived for α Boo with those derived from Williams and Hiltner's atlas (horizontal scale).

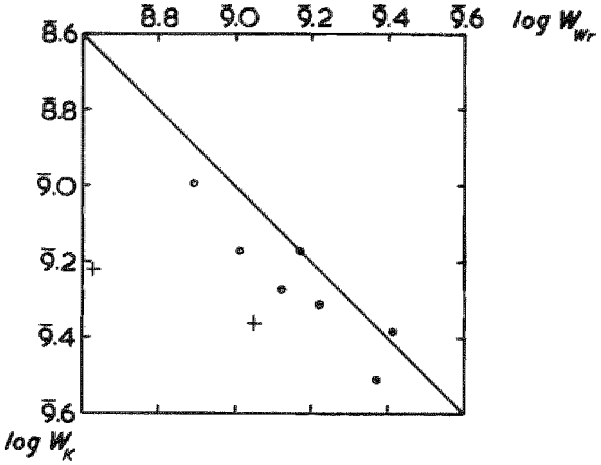

Fig. 4. Comparison of line intensities, derived for α Boo, with the measurements of K. O. Wright (horizontal scale).

of atomic weight and wave length. Apart from a constant factor for a given element, these Nf values may also be used for the stars in a first approximation, treated in the present Chapter. Modern analysis shows that N is a complicated function of the ionization and excitation potential and of the model of the atmosphere[39], which will be considered in Chapter III. The use of solar Nf-values we are about to make may be criticized, but in view of the limited accuracy of the observed intensities, the procedure is thought to be sufficient for a first approach. The curves of growth for *Fe* I were constructed in the manner described below. For more details of the method, we refer to section 13. The solar Nf-values were reduced to the number in the ground state, with the help of the Boltzmann formula (6a) of section 13, adopting a plausible value for the temperature difference with the sun. These reduced log Nf-values were plotted against the observed log W/λ for the star, and a preliminary curve of growth was thus constructed. Then the remaining systematic horizontal displacements of the multiplets of different excitation potential, relative to the curve of growth, were derived and used for the computation of a temperature correction, in order to obtain a stellar curve of growth *with a minimum spread of points* valid for the ground state. The corrected temperature difference is used in the Boltzmann formula to obtain the final Nf-values, reduced to the ground state.

The resulting curves of growth for *Fe* I are represented in the figures 5—9. The crosses indicate mean values. Although the faint lines are few, the transition to the Doppler branch is apparent for α Boo, 70 Oph and 61 Cyg. For the giant α Tau and the supergiant ξ Cyg the transition is difficult to detect owing to the spread of the points. A larger dispersion is urgently needed in these cases to obtain fainter lines. The damping part of the curves is well represented in all our stars.

Owing to the small number of atomic lines measured of the other elements and of the ion lines of all elements, the same shape for their curves of growth as derived for *Fe* I, and also the same excitation temperature must be adopted. Only horizontal shifts, according to a different degree

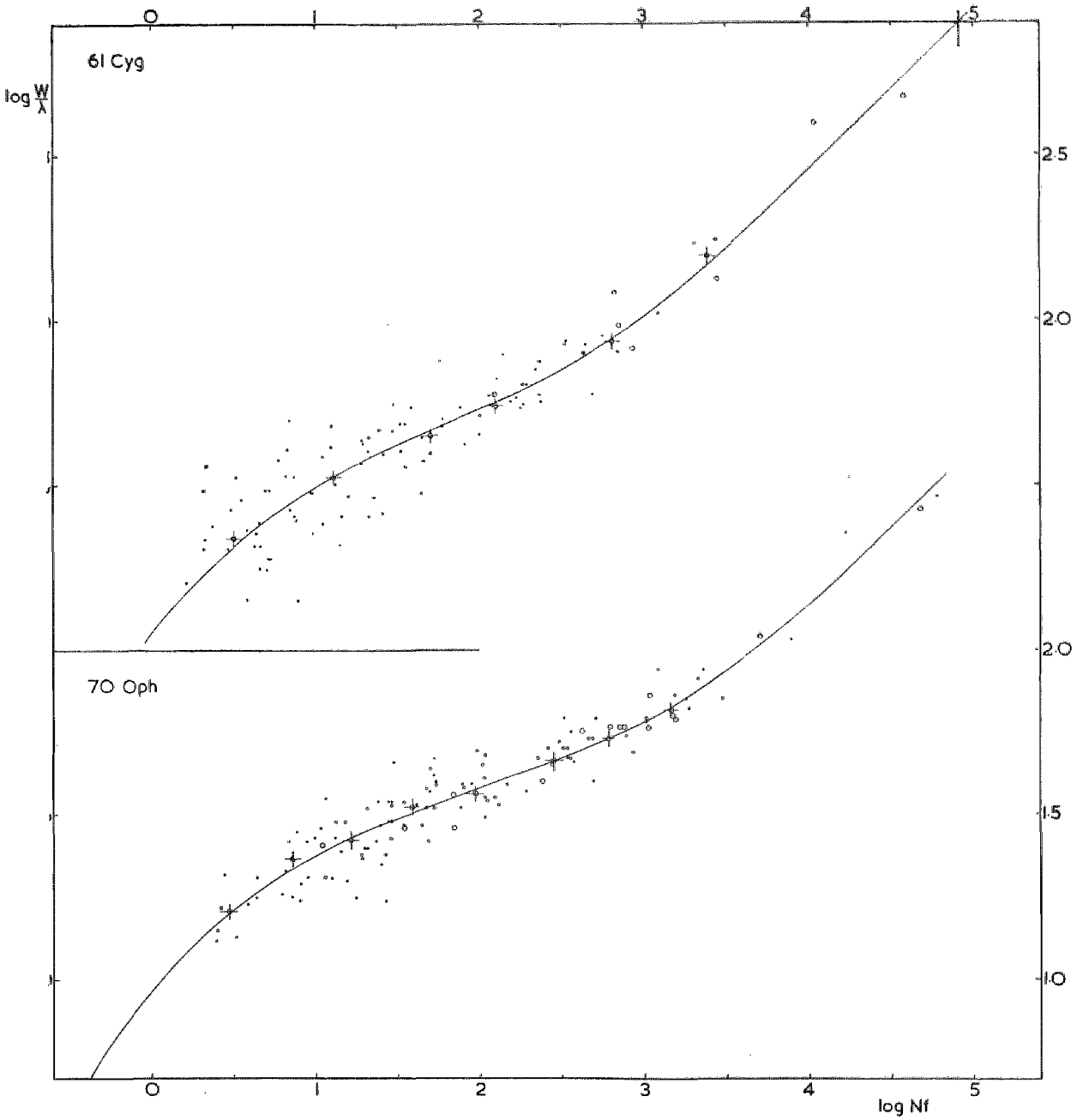

Fig. 5—6. Curves of growth for the *K* dwarfs. *Fe I* lines only. Spectral region $\lambda\lambda$ 4315—4770 A for 61 Cygni and $\lambda\lambda$ 4237—4770 A for 70 Ophiuchi. The crosses are mean values. Full lines are Wrubel's theoretical curves of growth.

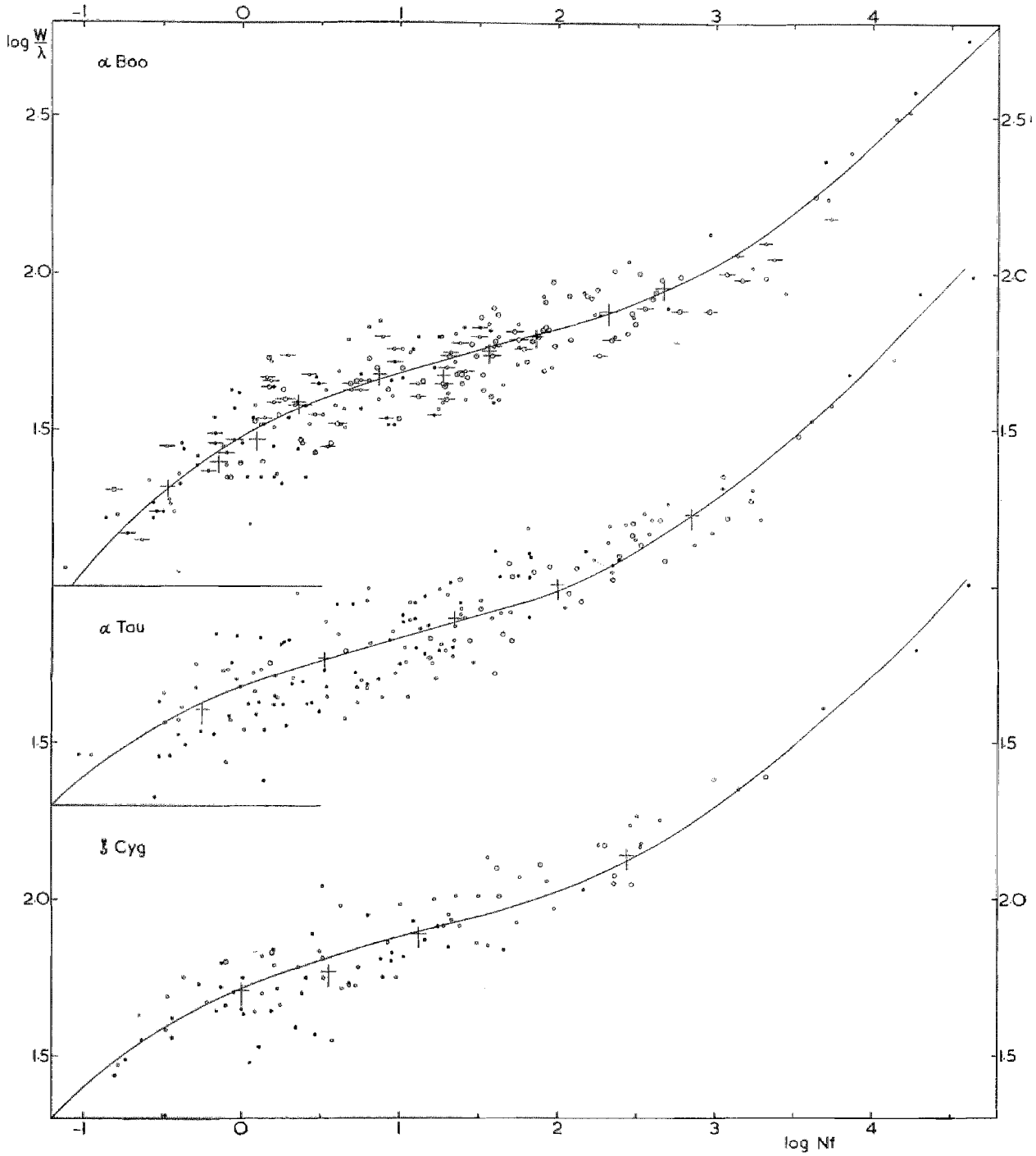

Fig. 7—9. Curves of growth for the *K* giants and *K* supergiant. *Fe I* lines only. Spectral region 4112—4770 for α Bootis and α Tauri, 4319—4770 for ξ Cygni. Crosses are mean values. For α Bootis the lines arising from odd lower terms are indicated as points with horizontal bars. Full lines are Wrubel's theoretical curves of growth.

of concentration are considered. Vertical shifts with respect to the *Fe*-curves, caused by different atomic weight, were thought to be of minor importance, owing to the turbulent velocity which turns out to be large.

We will now compare these results with theoretical curves of growth. A priori, we do not know the structure of the stellar atmospheres. So it is not easy to decide if the Milne-Eddington or the Schuster-Schwarzschild model is to be preferred for the bulk of the lines. Since in some respect the models are extremes, the difference of the results, in using both types, will give some idea of the uncertainties of the derived data.

For the theoretical curves of growth, based on the Milne-Eddington model, we have chosen the curves computed by Wrubel[37] for $B^\circ/B^1 = 1/3$. The B's are the coefficients in the expression for the Planck temperature function $B(T)$ expressed as a linear function of the optical depth in the continuum.

$$B_\nu(T) = B^\circ + B^1\tau_\nu$$

Expanding $B_\nu(T)$ by a Taylor's series, we get

$$B^\circ/B^1 = \frac{8}{3}\frac{k}{h}\frac{T}{\nu}\frac{\varkappa_\nu}{\bar{\varkappa}}$$

For the middle part of our spectral region, taking $\frac{\varkappa_\nu}{\bar{\varkappa}} = 1$, we have for the sun $B^\circ/B^1 = 0.41$ and for α Bootis 0.26. Adopting for the K stars, as in the sun, the H^- ion as the chief agency of the continuous absorption, and considering the uncertainties about the actual ratio of $\frac{\varkappa_\nu}{\bar{\varkappa}}$, we take for the sun and the K stars $B^\circ/B^1 = 1/3$. Comparing Wrubel's curves for $B^\circ/B^1 = 1/3$ and $2/3$, we note that the form of the whole set of curves for both values is practically the same. Only a very small shift in the horizontal direction is perceptible. Also in view of the problematic validity of the linear approximation for B_ν, it seems legitimate to use the same set of curves for all our K stars. As the spectral region is small, no corrections for different wave lengths are applied.

In figures 5—9 the theoretical curves of growth (Wrubel) are drawn after a horizontal and vertical shift, so that the mean values of the observed points, indicated by crosses (+), lie on the curve as well as possible. For the giant α Tau and the supergiant ξ Cyg the reasonable assumption $\Delta\lambda_N = \Delta\lambda_{N_{cl}}$ was made, as the transition to the Doppler branch is uncertain. No definite deviations of the observed curves from the theoretical forms can be established. It must be remarked that Allen's curves for the sun fit also very well on these theoretical curves.

The parameters deduced from the comparison are given in table 9. Our observed curve of growth has the vertical coordinate log W/λ, Wrubel's vertical, coordinate is log $W/\Delta\lambda_D$, so that the difference in zero point is $\Delta\lambda_D/\lambda$. The resulting $\Delta\lambda_D$ is given in column 4 (M.E.).

We also compared our observed curves of growth with Unsöld's curves (Physik der Sternatmosphären p. 268) based on the S.S-model, taking $R_c = 1$. As is seen from our table all Doppler widths $\Delta\lambda_D$ are smaller (mean $\Delta \log \lambda_D = 0.07$) for the S.S-model. This effect is often found[34, 35]. In column 5 we give the turbulent velocity V_t in km per sec., as found from the mean of columns 3 and 4, after correcting with formula (2) for the temperature, given in table 19, columns 8 and 9.

Table 9.

Star	Spectrum	Mean λ	log $\Delta\lambda_D$		V_t in km/sec	log a	$\Delta\lambda_N/\Delta\lambda_{N_{cl}}$
			M.E.	S.S.			
α Boo	$gK2$	4360	8.77	8.66	3.4	— 3.00	1.0
α Tau	$gK5$	4400	8.85	8.83	4.7	(— 3.08)	1.0 (adopted)
ξ Cyg	$cK4$	4500	8.89	8.83	4.7	(— 3.12)	1.0 (adopted)
70 Oph	$dK1$	4480	8.63	8.59	2.5	— 2.41	2.8
61 Cyg	$dK5$	4480	8.75	8.63	3.1	— 2.00	9.5

The giants have larger turbulent velocities than the dwarfs. The turbulent velocity of 61 Cygni seems high for a normal dwarf.

The value of $\log a = \log (\Delta\lambda_N/\Delta\lambda_D)$ is derived from the upper part of Wrubel's M.E. curves of growth in coincidence with our experimental points and the column 8 contains the ratio of the damping width $\Delta\lambda_N$ to its value for a classical oscillator $\Delta\lambda_{N_{cl}}$ (2*b*). For the giant α Boo the classical value of the radiation damping is found, as was expected. The dwarf 61 Cygni behaves in this respect as the sun, whereas 70 Oph. seems to have somewhat smaller damping.

The a values derived with both models are nearly identical. The position of the Doppler asymptote, which is the asymptote to the curve of growth for very faint lines, is the same with respect to the middle and the upper part of the curves, independent of the model. For the lower part, Unsöld's curves are nearer to the asymptote than those of Wrubel. According to Van Albada[15], Unsöld's curves give too large equivalent widths for the faint lines. So, for the determination of the Doppler asymptotes the M.E. curves were preferred. The horizontal displacement of the Doppler asymptotes with regard to the solar asymptote gives the $\Delta \log N = \log N_* - \log N_\odot$ for the ground state of the element considered. For the atoms and ions of iron and titanium the Δ log N's are given in table 10. These values will be used in Chapter 14 to obtain ionization temperature and electron pressure.

The mean errors are computed from a least square solution of formula (6a) of section 13. It is supposed that the error in $\Delta\ \theta_{exc}$, found there from the *Fe* I lines, is the same for the other cases. The true mean errors in Δ log N will be *larger*, chiefly because of the uncertainty of the reduction to faint lines, but also because of possible systematic differences in turbulent velocities of atoms and ions and of different elements. For α Tau and ξ Cygni an error may be introduced by the assumption of classical damping. For the latter star no reliable *Fe* II lines are found.

Table 10. Δ log N (star-sun).

	α Boo	α Tau	ξ Cyg	70 Oph.	61 Cyg.
Fe	2.17 ± 0.09	2.74 ± 0.13	2.72 ± 0.12	1.13 ± 0.10	1.20 ± 0.09
Fe^+	1.58 ± 0.19	2.08 ± 0.30	— —	0.44 ± 0.20	0.04 ± 0.30
Ti	2.26 ± 0.07	2.88 ± 0.11	2.78 ± 0.16	1.14 ± 0.10	1.68 ± 0.08
Ti^+	1.76 ± 0.11	2.21 ± 0.15	2.40 ± 0.16	0.73 ± 0.10	0.22 ± 0.18

11. THE CARTER EFFECT.

In constructing a curve of growth for the sun, using laboratory f values, determined photoelectrically, Carter[36] noted that lines with odd lower terms were lying on the damping branch systematically higher than those with even lower terms. As he did not find such differences in supergiant F stars, he supposed the effect to be caused by the higher pressure in the solar atmosphere. As we used solar Nf values for the stars, we may then expect for the giant stars, with their smaller pressure, an inverse position of the points for both types of lines on the damping branch of the stellar curve of growth. Carter found such an indication in the curve of growth of δ Cephei, constructed with solar Nf values by Walraven[2]. Such an inversion seems to be feebly present in our curve of growth for Arcturus, where the lines with odd lower terms are indicated as points with horizontal bars.

For ξ Cygni, no "odd" lines are lying on the damping branch, therefore no conclusion can be drawn about this question for this supergiant. Wright[13] recently found for the giants α Boo and γ Dra similar effects as Carter found for the sun. An explanation by means of pressure effects becomes difficult then. If Wright is correct the effect of inversion reported above will be minimized, if solar Nf values were used for the stellar cases.

The problem becomes complicated by the fact that, for the lines used, the odd lower terms have, on the average, a higher excitation potential than the even lower terms. Therefore the results for the excitation temperature may be affected by this effect. Also stratification effects may complicate the problem.

The Carter effect should certainly have some influence on the spread of the points in our curves of growth. However, no quantitative data exist to correct the place of the points.

12. COMPARISON OF CURVES OF GROWTH WITH THE RESULTS OBTAINED BY OTHER OBSERVERS.

Only for Arcturus and 70 Oph. comparison with other publications is possible. Miss van Dijke[12] published for both stars curves of growth for *Fe* lines, lying in the ordinary photographic spectral region. For Arcturus her result of 3.25 km/sec for the turbulent velocity agrees with our 3.4 km/sec. For the mean damping constant of the iron lines in this star, we obtained a value equal to the classical damping constant, whereas her observations agree with a value twice as large. She gives Δ log N values for atoms and ions for α Boo and 70 Oph. Her estimates are collected in table 11, together with the differences with our table 10 (last column).

Table 11. Comparison of Δ log N with the results obtained by Miss van Dijke.

	α Boo.		70 Oph.	
	Δ log N (van Dijke)	Δ	Δ log N (van Dijke)	Δ
Fe	1.94	+ 0.23	0.53	+ 0.60
Fe^+	1.24	+ 0.34	0.13	+ 0.31
Ti	2.51	— 0.25	0.75	+ 0.39
Ti^+	1.59	+ 0.17	0.45	+ 0.28
mean		+ 0.12		+ 0.40

It should be noted that she used also Allen's solar intensities, but another solar curve of growth (of K.O. Wright) for obtaining solar Nf values.

Considering the different treatment and the differences in dispersion (2.9 A/mm for Van Dijke, 10 A/mm for Koelbloed) the systematic differences for α Boo are small. For 70 Oph our A log N's are systematically larger. These differences may be partly explained by her less exact method of calibration, which does not preclude the possibility of a systematic error in log W for that star.

Wright[13] recently published an important study of the curve of growth of α Boo, in the spectral region 4656—6743 A. For lines with lower even terms he gives for *Fe* the damping width 1.3 times the radiation damping constant. Our value of equality is based on the same type of lines. As these lines are of low excitation potential and as it is believed that the Carter effect is small for low excitation, our damping branch, derived from solar Nf values, is probably insignificantly affected by the Carter effect.

For the turbulent velocity of the iron atoms Wright finds a somewhat lower value of 2.7 km/sec. against our 3.4 km/sec.